STEM CELLS
TRANSLATIONAL MEDICINE®

TISSUE ENGINEERING AND REGENERATIVE MEDICINE

Adipose Stromal Cells Repair Pressure Ulcers in Both Young and Elderly Mice: Potential Role of Adipogenesis in Skin Repair

AMY L. STRONG,[a] ANNIE C. BOWLES,[a] CONNOR P. MACCRIMMON,[a] TRIVIA P. FRAZIER,[a] STEPHEN J. LEE,[a] XIYING WU,[b] ADAM J. KATZ,[c] BARBARA GAWRONSKA-KOZAK,[d] BRUCE A. BUNNELL,[a,e] JEFFREY M. GIMBLE[a,b,f,g,h]

Key Words. Adipose • Adult stem cells • Mesenchymal stem cells • Stem cells • Stromal cells • Wound healing

[a]Center for Stem Cell Research and Regenerative Medicine and [e]Department of Pharmacology, Tulane University School of Medicine, New Orleans, Louisiana, USA; [b]LaCell LLC, New Orleans, Louisiana, USA; [c]Division of Plastic and Reconstructive Surgery, Department of Surgery, University of Florida, Gainesville, Florida, USA; [d]Institute of Animal Reproduction and Food Research of Polish Academy of Sciences, Olsztyn, Poland; Departments of [f]Medicine, [g]Surgery, and [h]Structural and Cellular Biology, Tulane Health Sciences Center, New Orleans, Louisiana, USA

Correspondence: Jeffrey Gimble, M.D., Ph.D., LaCell LLC, 1441 Canal Street, Suite 304, New Orleans, Louisiana 70112, USA. Telephone: 504-598-5246; E-Mail: jeffrey.gimble@ lacell-usa.com

ABSTRACT

More than 2.5 million patients in the U.S. require treatment for pressure ulcers annually, and the elderly are at particularly high risk for pressure ulcer development. Current therapy for pressure ulcers consists of conservative medical management for shallow lesions and aggressive debridement and surgery for deeper lesions. The current study uses a murine model to address the hypothesis that adipose-derived stromal/stem cell (ASC) treatment would accelerate and enhance pressure ulcer repair. The dorsal skin of both young (2 months old [mo]) and old (20 mo) C57BL/6J female mice was sandwiched between external magnets for 12 hours over 2 consecutive days to initiate a pressure ulcer. One day following the induction, mice were injected with ASCs isolated from congenic mice transgenic for the green fluorescent protein under a ubiquitous promoter. Relative to phosphate-buffered saline-treated controls, ASC-treated mice displayed a cell concentration-dependent acceleration of wound closure, improved epidermal/dermal architecture, increased adipogenesis, and reduced inflammatory cell infiltration. The ASC-induced improvements occurred in both young and elderly recipients, although the expression profile of angiogenic, immunomodulatory, and reparative mRNAs differed as a function of age. The results are consistent with clinical reports that fat grafting improved skin architecture in thermal injuries; the authors of this published study have invoked ASC-based mechanisms to account for their clinical outcomes. Thus, the current proof-of-principle study sets the stage for clinical translation of autologous and/or allogeneic ASC treatment of pressure ulcers. STEM CELLS TRANSLATIONAL MEDICINE 2015;4:1–11

SIGNIFICANCE

Adipose-derived stromal/stem cells (ASCs) promote the healing of pressure ulcer wounds in both young and old mice. ASCs enhance wound healing rates through adipogenic differentiation and regeneration of the underlying architecture of the skin.

INTRODUCTION

Pressure ulcers afflict 11% of American nursing home residents, and 70% of all pressure ulcers occur in subjects >70 years of age [1]. As the average life span increases nationally and internationally, the number of elderly individuals at high risk of pressure ulcers will grow substantially in the coming years [1]. The risk of pressure ulcers is not limited to the elderly but includes younger patients with paraplegia or quadriplegia secondary to spinal cord trauma caused by automobile accidents, gunshot wounds, or blast injuries. Based on the prevalence of 755 cases per million individuals, it is estimated that 250,000 quadriplegic patients are hospitalized annually in the U.S. [2].

Epidemiological studies have determined that nearly 40% of spinal cord injury patients experience a pressure ulcer and that those who require surgery are at a 20% increased rate of mortality [3, 4].

Pressure ulcers compromise the integrity of the epidermis, dermis, and underlying adipose tissue, muscle, and bone [5]. The current standard of care for pressure ulcers relies on traditional surgical debridement, negative pressure wound therapy (or other wound care methods/dressings), flap reconstruction, hyperbaric oxygen, bioengineered skin substitutes, and negative pressure devices to drain fluid exudates; local delivery of growth factors remains an experimental adjunct [6–9]. Risk factors for

pressure ulcers include conditions that deteriorate with advanced age such as loss of subcutaneous adipose tissue, loss of sensation, thinning skin, edema, immobility, impaired circulation, incontinence, infection, and malnutrition [1, 9].

Although the fundamental mechanisms responsible for healing in pressure ulcers are not fully understood, skin injury models provide valuable clues. Studies suggest that repeated cycles of ischemia reperfusion, impairing blood and lymph flow locally, lead to cell necrosis in the epidermis, dermis, subcutaneous adipose, and skeletal muscle tissues [10–12]. Prior preclinical pressure ulcer studies have used a variety of rodent models including the diabetic mouse [13–19], and only two murine studies have examined the effect of age on healing outcomes [16, 20]. In one study, chitosan scaffolds with or without fibroblast growth factor 2 were found to accelerate the closure of pressure ulcer wounds in old (20–22 months old [mo]) mice [16]. In a second study examining bone marrow stromal/stem cells, investigators found that bone marrow-derived lineage depleted Sca-1-positive cells obtained from young donors (2–3 mo) increased wound closure rates and angiogenesis in wild-type and leptin receptor-deficient obese diabetic mice [20]. Similar lineage depleted Sca-1-positive cells obtained from older (20–24 mo) mice were found to inhibit wound repair [20]. This study suggests that stromal/stem cells from young donors may improve pressure ulcer wounds, whereas stromal stem cells from older donors may inhibit healing. Unlike bone marrow, adipose tissue is an abundant and readily accessible organ that yields an estimated 10- to 1,000-fold more stromal/stem cells per unit volume of harvested tissue [21]. Adipose-derived stromal/stem cells (ASCs) secrete paracrine factors such as hepatocyte growth factor (HGF) and vascular endothelial growth factor (VEGF) that contribute to angiogenesis and vascularization [22]. These, in turn, promote repair and remodeling mechanisms. Multiple independent studies have documented the ability of ASCs to secrete cytokines capable of promoting tissue regeneration [23, 24]. In light of this background, the current translational studies were designed to generate proof-of-principle data, establishing the ability of ASC to accelerate and enhance wound healing in a murine pressure ulcer model. The described outcomes suggest that ASC-based therapies will have considerable impact on pressure ulcer treatment in high-risk elderly, as well as younger individuals.

MATERIALS AND METHODS

Materials

Collagenase type I was purchased from Worthington Biochemical Corporation (Lakewood, NJ, http://www.worthington-biochem. com). Bovine serum albumin, dexamethasone, β-glycerophosphate, ascorbate-2-phosphate, $1\alpha,25$-dihydroxyvitamin D$_3$, HEPES, biotin, pantothenate, insulin, 1-methyl-3-isobutylxanthine, rosiglitazone, Oil Red O, alizarin red, crystal violet, H_2O_2, neutral buffer formalin, HistoChoice, Tris-HCl, NaCl, and Permount mounting medium were purchased from Sigma-Aldrich (St. Louis, MO, http:// www.sigmaaldrich.com).

Rabbit anti-mouse CD29, rabbit anti-mouse CD31, rabbit anti-mouse CD34, rabbit anti-mouse CD45, rabbit anti-mouse CD11b, rabbit anti-mouse Sca-1, and isotype-control mouse IgG1 were purchased from eBiosciences (San Diego, CA, http://www. ebioscience.com). Rabbit anti-mouse green fluorescent protein (GFP), mouse anti-mouse pancytokeratin, and goat anti-mouse

perilipin primary antibodies were purchased from Abcam (Cambridge, MA, http://www.abcam.com). Goat anti-rabbit horseradish peroxidase (HRP)-conjugated, rabbit anti-mouse HRP-conjugated, and rabbit anti-goat HRP-conjugated secondary antibodies were purchased from Abcam.

Animals

Female C57BL/6 wild-type mice (2 and 20 mo) were purchased from Charles River Laboratories (Wilmington, MA, http://www. criver.com). All mice were healthy and were allowed to acclimate for at least 1 week prior to the induction of pressure ulcers via magnet application. For the isolation of stromal vascular fraction (SVF) and expansion of ASCs, male and female C57BL/6-Tg(UBC-GFP)30Scha/J mice were purchased from Charles River Laboratories and bred at Tulane University. All mice were housed in specific pathogen-free facilities, monitored regularly for illness, and provided with food and water ad libitum. All studies and procedures involving animals were conducted in compliance with guidelines established by Tulane University Institutional Animal Care and Use Committee (IACUC) and were approved by the Tulane University IACUC.

Isolation and Expansion of GFP-Positive ASCs

ASCs were isolated from inguinal white adipose tissue harvested from transgenic C57BL/6-Tg(UBC-GFP)30Scha/J mice under an approved IACUC protocol. Collected fat tissue was weighed, minced, and digested in (wt/vol) phosphate-buffered saline (PBS; HyClone, Logan, UT, http://www.hyclone.com; Thermo Fisher Scientific, Waltham, MA, http://www.thermofisher.com) supplemented with 0.1% collagenase type I and 1% bovine serum albumin for 1 hour in a shaker incubator set to 100 rpm at 37°C. After digestion, tissue was neutralized with complete culture medium (CCM, vol/vol) and centrifuged at 300g for 5 minutes. CCM consisted of Dulbecco's modified Eagle's medium/Ham's F-12 medium, 10% fetal bovine serum (HyClone), and 1% penicillin/ streptomycin (Gibco, Grand Island, NY, http://www.invitrogen. com; Life Technologies, Rockville, MD, http://www.lifetech. com). Pelleted SVF cells were resuspended in 25 ml of CCM and plated on T175 flasks (CellStar; Greiner Bio-One, Monroe, NC, http://www.gbo.com/en) and allowed to adhere for 48 hours at 37°C with 5% humidified CO_2. Adherent ASCs were washed with PBS, and fresh CCM was replaced every 2–3 days until cells achieved 70% confluence for expansion. When 70% confluent, viable cells were harvested with 0.25% trypsin, 1 mM EDTA (Gibco) and prepared for injection. For all experiments, subconfluent cells ($\leq$ 70% confluent) between passages 0 and 3 were used.

Characterization of GFP$^+$ ASCs: Morphology, Cell Surface Marker Profile, Differentiation, and Colony-Forming Units

Prior to injection of GFP-positive (GFP$^+$) ASCs into wounds, cells were characterized by morphology, cell surface marker profile, differentiation, and capacity to generate colony-forming units as previously described [25, 26]. Briefly, ASCs were induced to undergo osteogenic and adipogenic differentiation. ASCs were cultured until 70% confluent, and medium was replaced with CCM containing osteogenic supplements, consisting of 10 nM dexamethasone, 10 mM β-glycerophosphate, 50 μg/ml ascorbate-2-phosphate, and 10 nM $1\alpha,25$-dihydroxyvitamin D$_3$. After 3 weeks, cells were fixed and stained with 40 mM alizarin red

(pH 4.1) to visualize calcium deposition. For adipogenic differentiation, ASCs were cultured until 70% confluent, and medium was replaced with CCM containing adipogenic supplements, consisting of 15 mM HEPES (pH 7.4), 33 μM biotin, 17 μM pantothenate, 10 nM insulin, 1 μM dexamethasone, 0.25 mM 1-methyl-3-isobutylxanthine, and 1 μM rosiglitazone. After 3 weeks, cells were fixed and stained with Oil Red O to detect neutral lipid vacuoles. Images for osteogenic differentiation were acquired at $\times$4 magnification, and images for adipogenic differentiation were acquired at $\times$10 magnification on Nikon Eclipse TE200 (Melville, NY, Japan, http://www.nikon.com) with a Nikon DXM1200F digital camera using Nikon ACT-1 software version 2.7.

To determine the self-renewal capacity of ASCs, cells were plated at a density of 100 cells on a 10-cm^2 plate in CCM. After 14 days, cells were stained with 3% crystal violet, and colonies greater than 2 mm in diameter were counted.

Analysis by flow cytometry of cell surface marker expression was conducted by resuspending 3×10^5 ASCs in PBS and staining with the following antibodies: anti-CD29, anti-CD31, anti-CD34, anti-CD45, anti-CD11b, anti-Sca-1, and isotype-control mouse IgG1. The samples were incubated for 30 minutes at room temperature, washed with PBS, and then analyzed with a Gallios flow cytometer (Beckman Coulter, Brea, CA, http://www.beckmancoulter.com) running Kaluza software (Beckman Coulter). At least 10,000 events were analyzed and compared with isotype controls. Gates were set so that no more than 0.1% of cells stained with isotype controls were positive.

Pressure Ulcer Model

The pressure ulcer model used was previously reported, and this study was conducted with slight modifications [14, 27]. Briefly, mice were placed under anesthesia using a mixture of isoflurane, oxygen was delivered by mask, and the hair on the dorsum was shaved. The dorsal skin was gently pulled up and placed between 2 circular 12-mm diameter magnets (Master Magnetics, Inc., Castle Rock, CO, http://www.magnetsource.com) for 12 hours and removed for 12 hours for 1 ischemia-reperfusion (IR) cycle. Mice were exposed to two IR cycles, resulting in 2 wounds per mouse after 2 days.

Delivery of ASCs

Wounds were treated with PBS or GFP$^+$ ASCs. GFP$^+$ ASCs (1.0×10^5, 2.5×10^5, or 1.0×10^6) were resuspended in a total volume of 100 μl of sterile PBS and injected subcutaneously into each wound with a 27-gauge 1/2-inch needle (Tyco Healthcare Group LP, Mansfield, MA, www.covidien.com) with a 1-ml Leur-Lok tip syringe (Becton, Dickinson and Company, Franklin Lakes, NJ, http://www.bd.com). All injections were performed under anesthesia, and each mouse received a total volume of 200 μl (100 μl per wound; two wounds per mouse). Each injection site was sealed with Vetbond tissue adhesive (3M, St. Paul, MN, https://solutions.3m.com) as needles were retracted.

Wound Assessment

Wounds were assessed for size and closure daily on shaved mice by blinded researchers after mice were shaved until the day of sacrifice. A digital carbon fiber caliper (Thermo Fisher Scientific) was positioned at the borders of the wounds to measure the length and width of each wound. Wound size was calculated based on the area of an ellipse: Radius of the length $\times$ Radius of the width $\times$ π.

Histological Examination and Immunohistochemistry

On the day of sacrifice, wounds were harvested with a 5-mm rim of unwounded skin tissue, fixed in 10% neutral buffer formalin for at least 48 hours, and embedded in paraffin. Formalin-fixed, paraffin-embedded (FFPE) skin sections (5 μm) were deparaffinized, rehydrated in HistoChoice and graded solutions of ethanol, and stained with hematoxylin and eosin (HE; Thermo Fisher Scientific) or Masson's trichrome stain (Poly Scientific R&D Corp., Avenue Bay Shore, NY, http://www.polyrnd.com) according to the manufacturer's instructions. Following staining, slides were dehydrated with graded solutions of ethanol and HistoChoice and sealed with Permount mounting medium (Thermo Fisher Scientific). Stained slides were scanned into a computer with ScanScope CS2 (Aperio, Vista, CA, http://www.leicabiosystems.com/pathology-imaging/aperio-epathology) using ImageScope software (Aperio).

Skin sections stained with HE were further assessed for depth of epidermis, dermis, subcutaneous layer, and muscle layer at the center of each wound. To measure the thickness of each layer, specific parameters were used based on location of layer and characteristics of the layer. The epidermis is the outermost layer of the skin and is composed of several layers of keratinocytes, giving the skin the appearance of a stratified squamous epithelium. Directly inferior to the epidermis is the dermis, which consists of connective tissue and provides strength and elasticity to the skin through collagen and elastic fibrils. The next layer below the dermis is the subcutaneous layer, which is composed of mature adipocytes, and inferior to the subcutaneous layer is the muscle layer composed of mature myocytes. To determine the percentage of each skin section occupied by resident mononuclear cells, an algorithm (ImageJ; National Institutes of Health, Bethesda, MD) was used to deconvolve the color information acquired with HE-stained slides, and the number of dark purple-colored pixels was quantified and represented as a percentage relative to the total number of pixels per skin section.

Skin sections stained with Masson's trichrome were further assessed for the percentage of collagen per skin section. An algorithm (ImageJ) was used to deconvolve the color information acquired with slides stained with Masson's trichrome, and the number of blue colored pixels was quantified and represented as a percentage relative to the total number of pixels per skin section.

FFPE skin sections were deparaffinized and rehydrated in HistoChoice and graded solutions of ethanol. Skin sections were quenched with 0.3% H_2O_2; rinsed with Tris-HCl:NaCl:Tween 20 (TNT), which consisted of 0.1 M Tris-HCl (pH 7.5), 0.15 M NaCl, and 0.05% Tween 20 (Invitrogen, Life Technologies); blocked with 1% bovine serum albumin; and stained with primary antibodies against GFP, pancytokeratin, or perilipin overnight at 4°C. Each skin section was subsequently washed in TNT buffer, incubated with appropriate secondary antibody for 1 hour at room temperature, and washed with TNT buffer. For colorimetric staining, slides were then incubated in 3,3'-diaminobenzidine (Vector Laboratories, Burlingame, CA, http://www.vectorlabs.com), washed with TNT, counterstained with hematoxylin (Thermo Fisher Scientific), and rinsed with deionized water. Slides were dehydrated in graded solutions of ethanol, followed by HistoChoice in the final

step, and sealed with Permount mounting medium. After staining, images were acquired at ×10 and ×40 with the ScanScope CS2 (Aperio).

RNA Isolation, cDNA Synthesis, and Quantitative RT-PCR

On the day of sacrifice, wounds (n = 3 per group) were harvested and trimmed to the edge of the wounds and homogenized for total cellular RNA extraction using a miRNeasy Mini Kit (Qiagen, Valencia, CA, http://www.qiagen.com) according to the manufacturer's instructions. RNA was then purified with DNase I digestion (Invitrogen) and reverse transcribed using the SuperScript VILO cDNA synthesis kit (Invitrogen). Quantitative real-time polymerase chain reaction (RT-PCR) was performed using the EXPRESS SYBR GreenER qPCR SuperMix Kit (Invitrogen) according to the manufacturer's instructions. Mouse primers were made against transforming growth factor β (TGF-β), VEGF, matrix metalloproteinase 9 (MMP-9), matrix metalloproteinase 13 (MMP-13), and β-actin (supplemental online Table 1). At the completion of the reaction, $\Delta\Delta C_t$ was calculated to quantify mRNA expression.

Statistical Analysis

The values are presented as means ± SD for in vitro analyses or means ± SEM for in vivo analyses. The statistical differences among two or more groups were determined by analysis of variance, followed by post hoc Tukey's multiple comparison tests. Statistical significance was set at $p < .05$. Analysis was performed using Prism 6.0 (GraphPad Software, Inc., San Diego, CA, http://www.graphpad.com).

RESULTS

Fundamental Differences Between Young and Old Skin at Baseline

To compare the histomorphologic appearance of skin from young and old mice at baseline, we studied mice that were 2 and 20 mo. Young skin displayed reduced inflammation and thicker collagen fiber bundles in the dermis compared with old skin (Fig. 1A). The dermis of old skin was characterized by the presence of open space interspersed with tangled, thin fibers, whereas young skin displayed a structured basket-weaving appearance (Fig. 1A). Aged skin also demonstrated reduced dermal thickness (140.5 ± 20.2 μm) compared with young skin (182.9 ± 18.5 μm; $p < .01$; Fig. 1B). No significant difference in the thickness of the other layers of the skin was observed between young and old skin (Fig. 1B). Assessment of the quality of the skin demonstrated enhanced resident mononuclear cells and reduced collagen deposition in aged skin compared with young skin (Fig. 1C, 1D). Analysis of the gene expression profile of young and old skin demonstrated a significant reduction in TGF-β, VEGF, and MMP-9 expression by 3.5-, 2.1-, and 4.2-fold, respectively in older mice (Fig. 1E). No significant difference in the transcript levels of platelet-derived growth factor β (PDGF-β), HGF, or MMP-13 was observed (Fig. 1E).

Characterization of ASCs

ASCs were isolated from the inguinal white adipose tissue of 6- to 12-week-old male and female mice. Prior to delivery of ASCs into mice to assess therapeutic efficacy, cells were characterized by microscopy, differentiation, colony formation capacity, and cell surface marker profile. ASCs displayed fibroblast-like morphology and expressed GFP visible by fluorescence imaging (Fig. 2A). The differentiation capacity of ASCs was assessed by culturing cells in adipogenic or osteogenic differentiation medium for 14 days and stained with Oil Red O and alizarin red, respectively. ASCs cultured in adipogenic differentiation medium displayed large neutral lipid vacuoles, whereas cells cultured in osteogenic differentiation medium demonstrated significant calcium deposition (Fig. 2B). These results demonstrate the adipogenic and osteogenic differentiation capacities of ASCs in inductive medium. Furthermore, ASCs plated at low density demonstrated the capacity to form colony-forming units (Fig. 2C). Immunophenotypic analysis of ASCs demonstrated expression of GFP, Sca-1, and CD29 on the cell surface (Fig. 2D). Although most of the ASCs were negative for CD31, CD11b, CD34, and CD45, a small subpopulation of ASCs (1%–5%) expressed these cell surface antigens (Fig. 2D).

ASCs Aid in Wound Healing in a Dose-Dependent Manner in Young Mice

The therapeutic dose of ASCs necessary to accelerate pressure ulcer wounds was investigated in young mice injected with different concentrations of transgenic GFP (GFP$^+$) ASCs (1.0×10^5, 2.5×10^5, and 1.0×10^6). Pressure ulcer wounds were assessed every 2 days (supplemental online Fig. 1). ASCs accelerated wound closure relative to PBS treatment (supplemental online Fig. 2; Fig. 3A). After 10 days, wounds treated with ASCs were smaller in size (1.0×10^5 ASCs = 42.7 mm^2; 2.5×10^5 ASCs = 43.3 mm^2; 1.0×10^6 ASCs = 22.3 mm^2) than wounds treated with PBS (55.9 mm^2; $p < .05$; Fig. 3A). Compared with lower concentrations of ASCs, higher concentrations of ASCs (1.0×10^6) delivered to the wound site further accelerated wound closure, suggesting that higher dosages of ASCs may be more efficacious at healing pressure ulcer wounds (Fig. 3A).

ASCs Accelerate Pressure Ulcer Wound Healing in Both Young and Old Mice

The efficacy of ASCs in pressure ulcer wounds was investigated in young and old mice by induction of pressure ulcers in 2- and 20-mo mice. A total of 1.0×10^6 ASCs were injected into the base of the wounds and assessed over 20 days (Fig. 3B, 3C; supplemental online Figs. 1, 3). Delivery of ASCs to the wound site accelerated wound healing in both young and old mice (Fig. 3B, 3C). As early as day 4, young mice treated with ASCs (67.2 mm^2) displayed smaller wounds compared with young mice treated with PBS (80.4 mm^2). The trend of ASC-accelerated wound size reduction continued until wound closure was completed on day 12 (Fig. 3B, 3C). Wounds induced in old mice also demonstrated accelerated wound healing after exposure to ASCs, compared with PBS-treated wounds, as early as day 6 (Fig. 3B, 3C). Furthermore, young mice treated with ASCs demonstrated accelerated wound healing compared with old mice treated with ASCs. These results suggest that although ASCs may enhance the wound healing rates, underlying differences are still apparent between the two groups after treatment (Fig. 3B, 3C). Interestingly, ASC-treated wounds resulted in repigmentation of the hair follicles over the wounds, whereas the PBS-treated wounds resulted in depigmented hair follicles (Fig. 3C).

ASCs Reduce Inflammation, Limit Hypertrophy, and Enhance Collagen Deposition

To assess the integrity of the skin, histomorphologic analysis was conducted on young and old skin harvested on days 5, 10, and 20
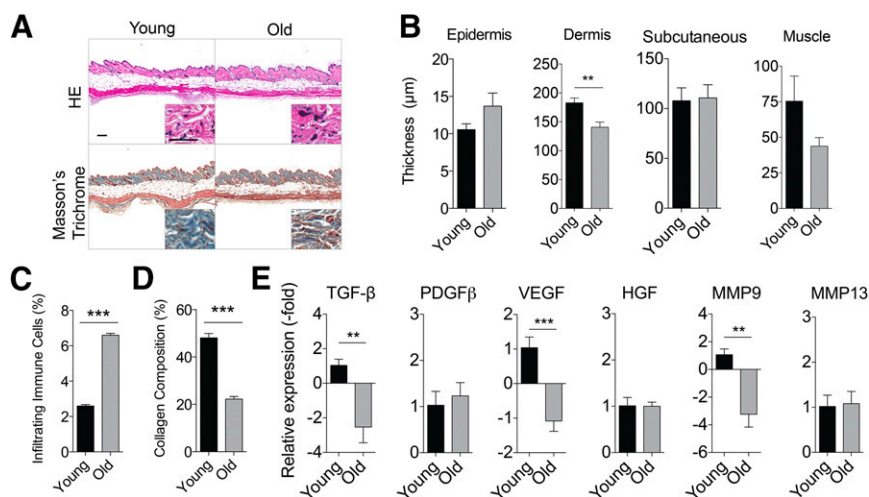
Figure 1. Aged skin displays reduced histological integrity and altered molecular profile compared with young skin. Healthy skin from young (2 months old, *n* = 5 mice) and old (20 months old, *n* = 5 mice) mice was collected. **(A):** Representative images of young and old skin stained with HE or Masson's trichrome. Scale bars = 200 μm. **(B):** Thickness of epidermis, dermis, subcutaneous tissue, and muscle layer of young and old mouse skin is shown (*n* = 5 mice per group; mean ± SEM). ∗∗, *p* < .01 **(C):** Resident mononuclear cells were assessed by color deconvolution followed by quantification of dark purple stain. **(D):** Collagen composition was assessed by color deconvolution followed by quantification of blue stain (mean ± SEM). ∗∗, *p* < .01; ∗∗∗, *p* < .001. **(E):** Young and old skin was analyzed by quantitative real-time polymerase chain reaction analysis. Data are normalized to young skin, set to 1.0 (mean ± SD). ∗∗, *p* < .01; ∗∗∗, *p* < .001. Abbreviations: HE, hematoxylin and eosin; HGF, hepatocyte growth factor; MMP, matrix metalloproteinase; PDGFβ, platelet-derived growth factor β; TGF-β, transforming growth factor; VEGF, vascular endothelial growth factor.
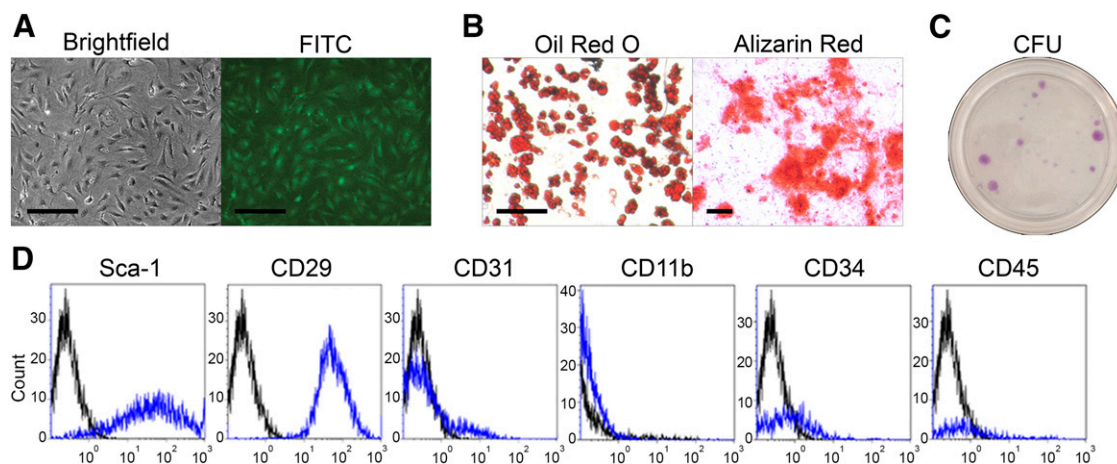

Figure 2. Characterization of GFP+ adipose-derived stromal/stem cells (ASCs). ASCs were cultured from the stromal vascular fraction of inguinal white adipose tissue harvested from green fluorescent protein-positive (GFP+) C57BL/6 mice, characterized, and injected into the dorsal skin of young mice with pressure ulcer wounds. **(A):** Representative images of culture expanded GFP+ ASCs viewed under bright field and fluorescence microscopy are shown. Scale bars = 200 μm. **(B):** GFP+ ASCs were cultured in adipogenic or osteogenic differentiation medium. After 21 days, cells were fixed and stained with Oil Red O for adipogenesis and alizarin red for osteogenesis. Representative images are shown. Scale bar = 200 μm. **(C):** Cells were seeded at low density and incubated in CCM for 14 days. Cells were fixed and stained with crystal violet. Representative images are shown. **(D):** GFP+ ASCs were stained with antibodies and analyzed by flow cytometry. Representative histograms are shown as blue lines, and respective isotype controls are shown as black lines. Abbreviations: CFU, colony-forming units; FITC, fluorescein isothiocyanate.

after PBS or ASC treatments. Young mice treated with ASCs demonstrated reduced infiltrating mononuclear cells compared with PBS after 5, 10, and 20 days (*p* < .05; Fig. 4A, 4B). Young mice with ASC-treated wounds (41.0 μm) demonstrated reduced epidermal hypertrophy compared with PBS-treated wounds (82.0 μm) on day 10 (*p* < .05; Fig. 4C). Likewise, young mice with wounds treated with ASCs (29.0 μm) demonstrated reduced epidermal hypertrophy compared with wounds treated with PBS on day 20 (89.0 μm; *p* < .01; Fig. 4C). On day 20, pressure ulcer wounds

in young mice treated with ASCs demonstrated similar thickness as normal skin, suggesting ASCs limit hypertrophy associated with PBS-treated wounds (Fig. 4C). ASCs increased the thickness of the dermis, subcutaneous adipose, and muscle layer of the skin on day 20, compared with PBS treatment (Fig. 4C). The data indicate that ASCs contributed to regeneration of the dermis, subcutaneous adipose, and muscle layers of the skin in young mice.

Histological analysis of old skin demonstrated significant differences between PBS-treated and ASC-treated pressure ulcer
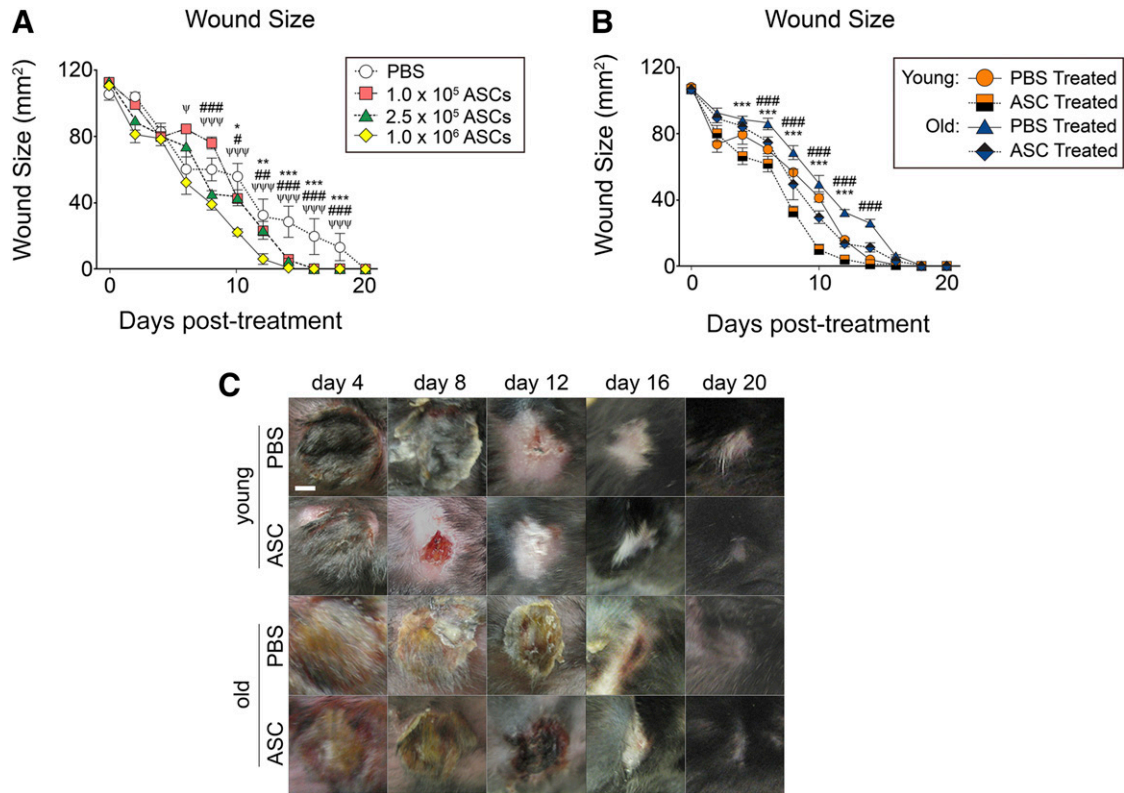
Figure 3. ASCs accelerate wound healing following pressure ulcer (PU) induction. **(A):** PU wounds were induced on the dorsal skin of mice ($n = 5$ mice per group) and treated with PBS, 1.0×10^5 ASCs, 2.5×10^5 ASCs, or 1.0×10^6 ASCs. Daily digital caliper measurements of the length and width of the wounds were acquired, and wound sizes are shown (bars, $\pm$SEM). $*$, $p < .05$; $**$, $p < .01$; $***$, $p < .001$ between PBS and 1.0×10^5 ASCs; #, $p < .05$; ##, $p < .01$; ###, $p < .001$ between PBS and 2.5×10^5 ASCs; ψ, $p < .05$; $\psi\psi$, $p < .01$; $\psi\psi\psi$, $p < .001$ between PBS and 1.0×10^6 ASCs. **(B):** Daily digital caliper measurements of the length and width of the wounds ($n = 5$) were acquired, and wound sizes are shown. **(C):** Representative images of treated wounds are shown (bars, $\pm$SEM). $*$, $p < .001$ between young PBS-treated and ASC-treated wounds. ###, $p < .001$ between old PBS-treated and ASC-treated wounds. Abbreviations: ASC, adipose-derived stromal/stem cells; PBS, phosphate-buffered saline.

wounds on days 5, 10, and 20. PBS-treated wounds demonstrated significant infiltrating mononuclear cells, whereas ASC treatment reduced the number of mononuclear cells in the skin section on days 5, 10, and 20 ($p < .05$; Fig. 4D, 4E). Wounds induced in old mice displayed greater percentage of infiltrating immune cells compared with young mice ($p < .05$; Fig, 4B, 4E). Epidermal and dermal hypertrophy was also reduced 20 days following delivery of ASCs, suggesting that ASCs immunomodulate the microenvironment of the wound (Fig. 4F). Subcutaneous adipose and muscle layers of the skin were restored following treatment with ASCs, whereas PBS-treated wounds lacked the subcutaneous adipose and muscle layers (Fig. 4F). In contrast to young skin, ASC treatment was unable to induce the regeneration of the subcutaneous adipose and muscle layer of skin. These results highlight the differences between young and old skin.

With respect to collagen deposition, ASC-treated wounds in both young and old mice displayed greater collagen deposition after 5 and 10 days (Fig. 5). By 20 days, no statistically significant difference was observed between PBS- and ASC-treated wounds in young or old mice (Fig. 5).

Activation of Reparative Genes by ASCs

During the reparative process, hemostasis followed by angiogenesis and keratinocyte migration occurs to heal the wound. The

molecular changes that occur within the wound following delivery of PBS or ASCs were assessed by harvesting wounds 5 days after treatment for comparison with normal skin. The mRNA expression of hemostatic factors (TGF-β, PDGF-β), angiogenic factors (VEGF, HGF), and matrix metalloproteinases (MMP-9, MMP-13) was analyzed. Relative to normal skin, the transcript levels of TGF-β, PDGF-β, VEGF, HGF, MMP-9, and MMP-13 expression was increased in young mice following PBS or ASC treatment by: 16.7- (PBS-treated) and 34.8-fold (ASC-treated) for TGF-β; 15.6- (PBS-treated) and 19.5-fold (ASC-treated) for PDGF-β; 57.8- and 112.2-fold for VEGF; 178.6- and 545.5-fold for HGF; 46.7- and 287.7-fold for MMP-9; and 19.9- and 87.6-fold for MMP-13 (Fig. 6A). ASC treatment enhanced the expression of reparative genes compared with wounds treated with PBS, which suggests that ASCs upregulate cytokines and other factors to aid in wound healing. In old mice, the expression of several reparative genes was likewise increased following PBS and ASC treatment: 73.1- (PBS-treated) and 44.8-fold (ASC-treated) increase for TGF-β; 9.8- (PBS-treated) and 20.2-fold (ASC-treated) increase for PDGF-β; 39.6- (PBS-treated) and 107.6-fold (ASC-treated) increase for VEGF; 57.2- (PBS-treated) and 151.1-fold (ASC-treated) increase for HGF; 108.4- (PBS-treated) and 499.6-fold (ASC-treated) increase for MMP-9; and 116.3- (PBS-treated) and 32.9-fold (ASC-treated) increase for MMP-13 (Fig. 6B).
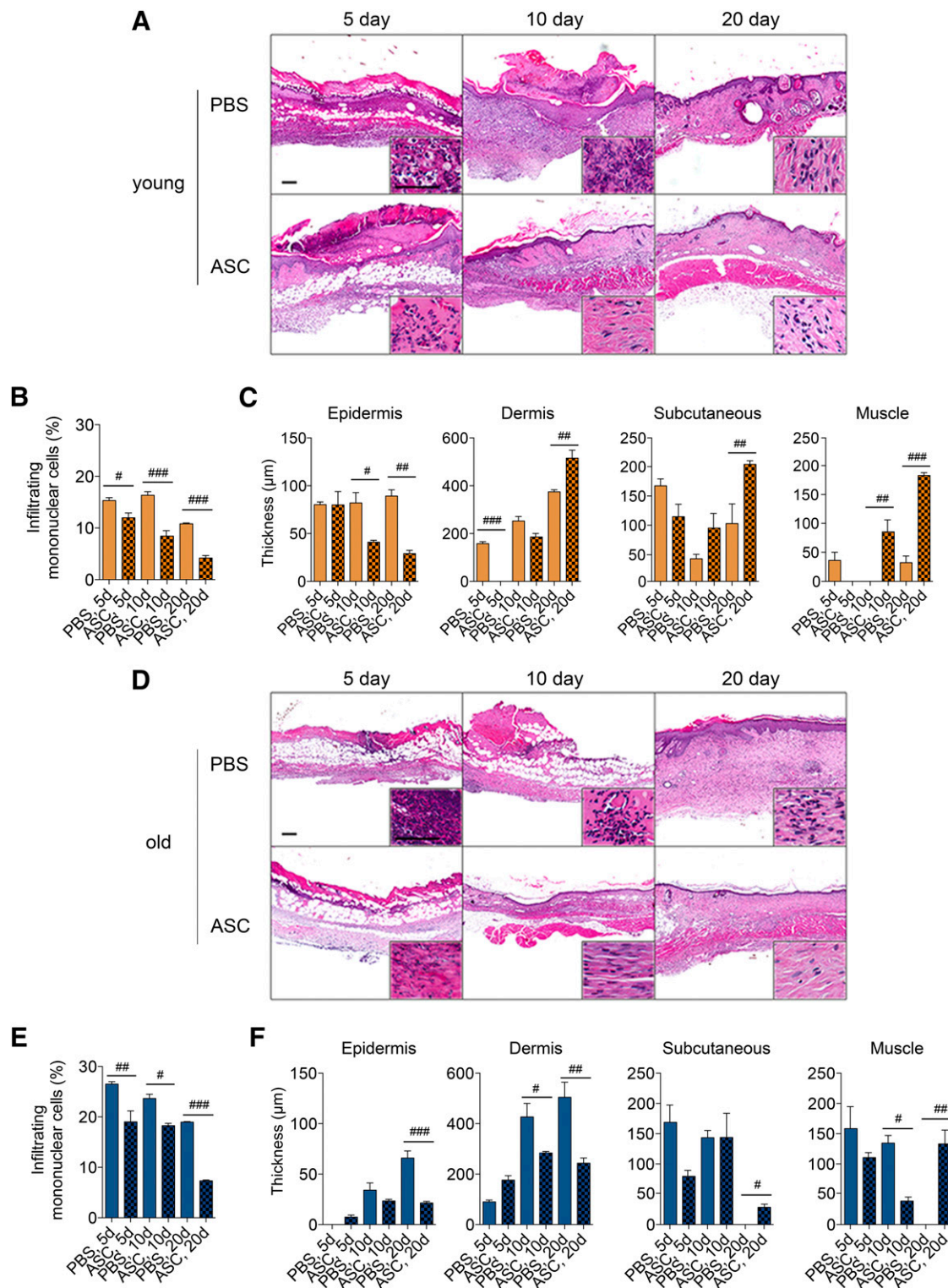
Figure 4. ASCs reduce inflammation and aid in regenerating the normal architecture of pressure ulcer (PU) skin in both young and old mice. PU wounds were induced on the dorsal skin of young (2 months old) and old (20 months old) mice. Wounds (*n* = 5 per group per day) were collected from young **(A–C)** and old **(D–F)** mice following PU induction and treatment with PBS or ASCs after 5, 10, and 20 days. **(A, D):** Representative images of skin sections stained with hematoxylin and eosin. Scale bars = 200 μm. Inset images were acquired from the dermal layers of the skin. **(B, E):** Infiltrating mononuclear cells were assessed by color deconvolution followed by quantification of dark purple stain. **(C, F):** Thickness of the epidermis, dermis, subcutaneous tissue, and muscle layers of skin (mean ± SEM). #, *p* < .05; ##, *p* < .01; ###, *p* < .001 between PBS-treated and ASC-treated wounds on the respective day. Abbreviations: ASC, adipose-derived stromal/stem cells; d, days; PBS, phosphate-buffered saline.
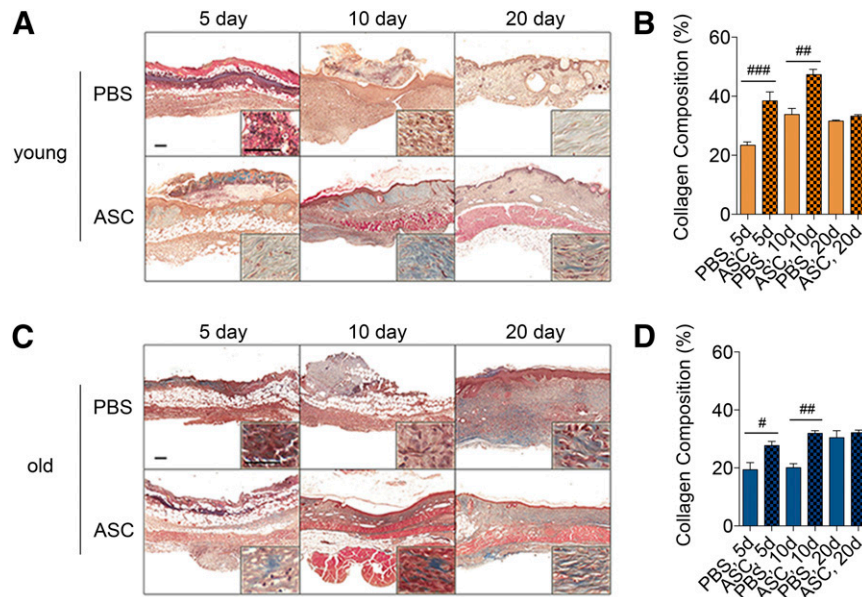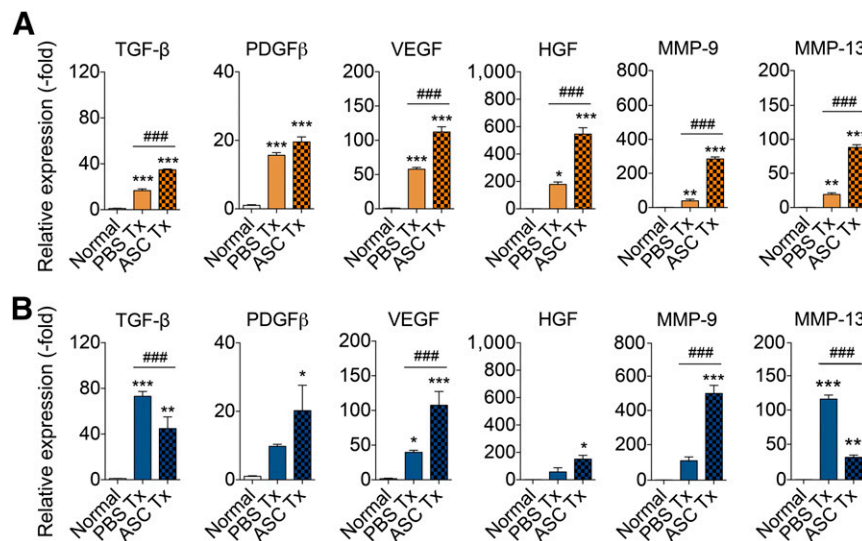
Figure 5. ASCs aid in restoring structural integrity and influence remodeling of pressure ulcer (PU) wounds in young and old animals. PU wounds were induced on the dorsal skin of young (2 months old) and old (20 months old) mice and treated with PBS or ASCs the day after PU induction. Wounded skin (*n* = 5 per group per day) was collected from young **(A, B)** and old **(C, D)** mice on days 5, 10, and 20. **(A, C):** Representative images of skin sections stained with Masson's trichrome. Scale bars = 200 μm. **(B, D):** Collagen composition was assessed by color deconvolution followed by quantification of blue stain (mean $\pm$ SEM). #, *p* < .05; ##, *p* < .01; ###, *p* < .001 between PBS-treated and ASC-treated wounds on the respective day. Abbreviations: ASC, adipose-derived stromal/stem cells; d, days; PBS, phosphate-buffered saline.

Figure 6. ASCs enhance expression of reparative genes to aid wound healing. Wounds were induced on the dorsal skin of young (2 months old) and old (20 months old) mice. Wounds (*n* = 3 per group per day) were harvested from young **(A)** and old **(B)** mice following pressure ulcer induction and treatment with PBS or ASCs after 5 days. Skin was analyzed by quantitative real-time polymerase chain reaction. Data are normalized to normal skin, set to 1.0 (mean $\pm$ SEM). *, *p* < .05; **, *p* < .01; ***, *p* < .001 between normal skin and treated wounds. #, *p* < .05; ##, *p* < .01; ###, *p* < .001 between PBS-treated and ASC-treated wounds. Abbreviations: ASC, adipose-derived stromal/stem cells; HGF, hepatocyte growth factor; MMP, matrix metalloproteinase; PBS, phosphate-buffered saline; PDGFβ, platelet-derived growth factor β; TGF-β, transforming growth factor; Tx, treatment; VEGF, vascular endothelial growth factor.

Differentiation of ASCs Into Epithelial Cells and Adipocytes

The fate of the ASCs after delivery into the wounds was investigated by harvesting wounds from young and old mice on post-treatment days 5 and 20. Sections were stained with antibodies against GFP, pancytokeratin, and perilipin to determine the fate of the cells. Five days after treatment, GFP expression was visible in the epidermal layer of young and old mice (Fig. 7A, 7B). The expression of GFP in epidermal layer was confirmed by pancytokeratin staining (Fig. 7A, 7B). By 20 days, GFP-positive cells were visible in the epidermal and subcutaneous adipose layer of the young and old skin. Interestingly, the GFP-positive cells were
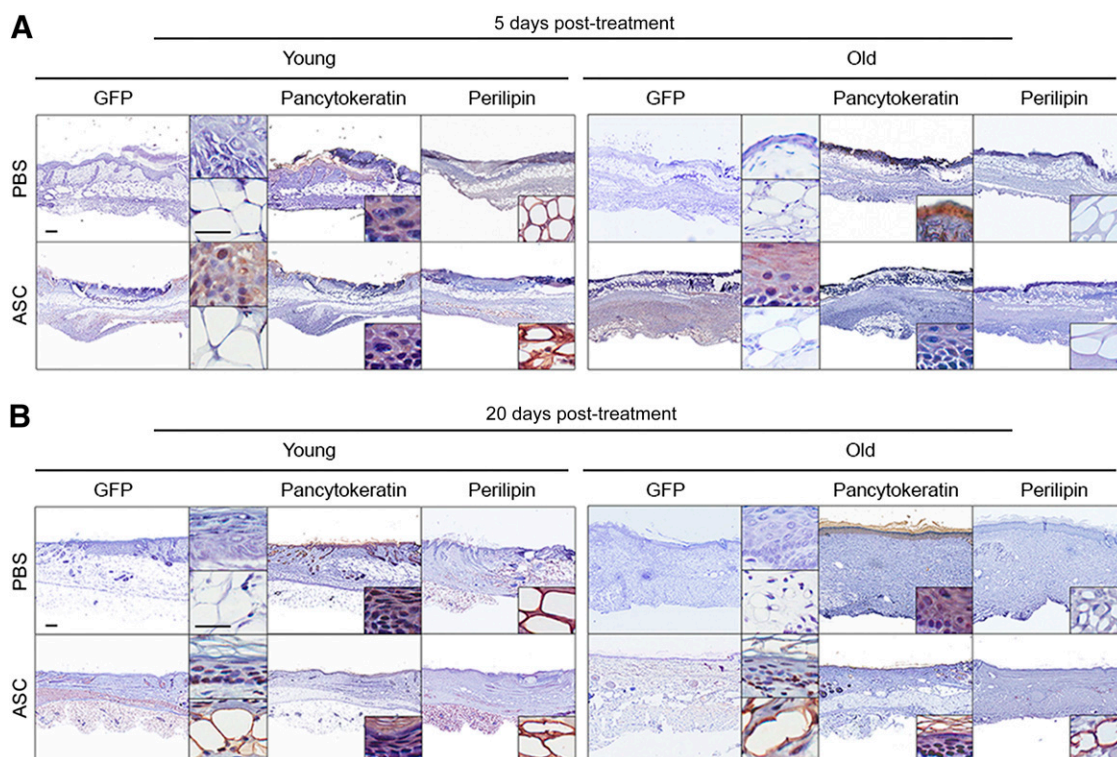
Figure 7. ASCs engraft into the wound site and differentiate into epithelial cells and adipocytes to aid in wound healing. Wounds were induced on the dorsal skin of young (2 months old) and old (20 months old) mice and treated with PBS or ASCs the day after pressure ulcer induction. Wounds ($n = 5$ per group per day) were collected from young and old mice on day 5 **(A)** and day 20 **(B)** and stained with antibodies detecting GFP, pancytokeratin, or perilipin. Scale bars = 200 μm. Abbreviations: ASC, adipose-derived stromal/stem cells; GFP, green fluorescent protein; PBS, phosphate-buffered saline.

visible at the base of the epidermis, which is proximal to epithelial stem cells located at the base of the epidermis (Fig. 7B). Furthermore, the presence of GFP expressing cells in the subcutaneous adipose layer confirmed by perilipin expression suggests differentiation of ASCs into mature adipocytes (Fig. 7B).

Safety of ASCs

To investigate the safety of ASCs, secondary organs were harvested from young and old mice on post-treatment day 20. Liver and lung tissue sections were stained with hematoxylin and eosin. Delivery of ASCs did not result in pathological findings in the liver or the lung (supplemental online Fig. 4). Differences were observed between young mice and old mice; however, these differences were attributed to aging. Old mice that received PBS and ASCs demonstrated poor structural integrity in both the liver and the lung compared with young mice that received PBS and ASCs, irrespective of the treatment group (supplemental online Fig. 4).

DISCUSSION

At present, treatment of pressure ulcers rely primarily on conservative medical management of less severe (stage I/II) pressure ulcers and surgical management of deeper pressure ulcers (stage III/IV) [9]. The prevalence of pressure ulcers in acute care settings ranges from 11% to 17% in the U.S. and exceeds 25% in Canada [28]. The elderly are at particularly high risk for pressure ulcer development because of age-related changes in subcutaneous tissue morphology, vascularization, and comorbidities leading to reduced mobility [9]. With the continued rise in average life span

throughout the world, the health care burden of pressure ulcers is expected to increase substantially. Consequently, there are demographic, economic, and medical arguments for the development of improved alternatives or adjunct pressure ulcer therapies.

A wealth of independent data over the past 15 years has unequivocally established adipose tissue as an abundant and rich source of stromal/stem cells with both multipotent and immunomodulatory characteristics [21, 29, 30]. The ASCs are similar to but not identical to bone marrow-derived multipotent stromal cells or mesenchymal stem cells (BMSCs) [31, 32]. In a study conducted by de la Garza-Rodea et al. [33], human BMSCs were ineffective at repairing pressure ulcers in excision skin wounds created in immunodeficient mice. In contrast, our study indicates that murine ASCs were effective at accelerating wound healing in immunocompetent syngeneic recipients. Clinical trials are under way using ASCs for regenerative medical and tissue engineering applications [34, 35]. Autologous ASCs have been used to repair craniofacial bone defects [36–38], and a phase I clinical trial recently reported the potential safety and efficacy of intramuscular ASC injection to treat critical limb ischemia [39]. In light of the recent U.S. Food and Drug Administration approval of allogeneic BMSCs (Prochymal) for the treatment of steroid-refractory graft versus host disease, there is increased confidence that ASCs and BMSCs will gain regulatory approval and increased clinical translation for the treatment of multiple conditions in the near future [40]. Furthermore, the absence of MHC class II molecules or costimulatory molecules indicate that ASCs have allogeneic uses. Studies conducted by our group and others have shown that ASCs isolated from old donors or from diseased mice are less efficacious

at healing pathological processes, such as wound healing, experimental autoimmune encephalomyelitis, and diabetes mellitus [20, 41–43]. Therefore, delivery of allogeneic ASCs from a young, healthy donor would lead to better outcomes because these cells should not induce an immune response and should lead to better efficacy.

Using a modification of an established murine pressure ulcer model [14, 27], the current study provides proof of principal data documenting the safety and efficacy of ASC therapy to accelerate and enhance wound repair in both young and elderly animals. The subcutaneous injection of GFP$^+$ ASCs into the base of pressure ulcers accelerated wound repair in both age groups. Furthermore, the injection of ASCs contributed to repigmentation of hair follicles, which is most apparent during the healing process in the young C57BL/6 mice on which the hair color changed from white to black. This intriguing observation suggests that ASCs with their adipogenic potential may contribute to or reinvigorate the dermal papilla mesenchymal cells, which are known to regulate the growth of hair follicles [44]; however, future studies will be necessary to explore the mechanism and role of ASCs in the process of hair growth and coloration.

A quantitative comparison of the histomorphologic data indicates that ASC-treated pressure ulcers display reduced levels of inflammatory cell infiltration relative to the PBS-treated counterparts independent of animal age, which suggests that the ASCs act in part via an immunomodulatory mechanism [30]. The ASC repair process demonstrates increased collagen deposition. Consistent with this finding, mechanical testing indicates that ASC treatment improves the tensile properties of the skin in both young and elderly mice relative to PBS-treated controls (C.P. MacCrimmon, S.J. Lee, A.L. Strong et al., manuscript in preparation). Additionally, the GFP$^+$ ASCs contribute to the growth and recovery of subcutaneous adipose tissue in both age groups. Mature GFP$^+$ adipocytes were evident in adipose tissue of both cohorts by 20 days. It remains to be determined whether the expression of secreted adipokines or other adipose-derived factors plays a direct role in pressure ulcer recovery. In parallel, there are time-dependent changes in the expression of genes associated with inflammation, as well as vascularization and cell migration during the repair process. In young mice, ASCs increased TGF-β and PDGF-β, which are necessary to induce an inflammatory response to initiate wound healing. Likewise, angiogenic genes were induced, and they may contribute to deliver nutrients to the healing skin. Increased levels of MMP-9 and MMP-13 were also observed, and they may contribute to immune cell or keratinocyte migration into the pressure ulcer site. In contrast, the TGF-β and MMP-13 expression levels of elderly mice were not higher in ASC-treated compared with PBS-treated wounds. Future mechanistic studies will require a systematic, time-dependent analysis of both the gene and protein expression profiles of pressure ulcer sites in ASC- and PBS-treated young and elderly mice.

The current study has similarities to alternative wound healing models. Amos et al. [23] found that diabetic mice with a circular full thickness excisional wound healed significant faster following treatment with multicellular ASC aggregates. ASC aggregates demonstrated higher production of extracellular matrix proteins and secretion of soluble factors, such as HGF, VEGF, EGF, and TGF-β, which may have aided in wound healing [23]. Independent studies using AZIP and *ob/ob* mice found adipocyte lineage cells to be critical to the repopulation of full thickness excisional skin wounds and re-epithelialization; these cells were required for the appearance of fibroblasts in the wound bed following skin wounding [45]. Consistent with this study, our study demonstrated that the introduction of exogenous ASCs enhanced re-epithelialization and repopulation of the wound with mature adipocytes.

CONCLUSION

The current findings support the hypothesis that ASCs can be used to accelerate and enhance pressure ulcer recovery in both young and elderly mice. This is in contrast to similar studies examining a full thickness skin wound model that failed to detect any benefit to ASC treatment in healthy young mice; ASC treatment accelerated wound repair only in mice with an underlying diabetic disease [23]. The mouse pressure ulcer model has practical utility as a starting point for clinical translation [14]; however, the architecture of human skin is unique, and no animal has gained universal acceptance as a "gold standard" experimental model [10]. Despite this limitation, the current findings are consistent with the clinical evidence. Plastic and reconstructive surgeons have noted improvements in skin architecture after using fat grafting to treat patients with radiation burns [46]. These authors have invoked a reparative role for transplanted ASCs as an underlying mechanism [46]. Although additional mechanistic and large animal translational studies are required, the current study builds on this clinical foundation by establishing proof-of-principle evidence for an ASC-based approach to pressure ulcer therapy.

AUTHOR CONTRIBUTIONS

A.L.S.: conception and design, collection and assembly of data, data analysis and interpretation, and manuscript writing; A.C.B., T.P.F., and S.J.L.: collection and assembly of data; C.P.M.: collection and assembly of data, data analysis and interpretation; X.W.: final approval of manuscript; A.J.K., B.G.-K., and B.A.B.: conception and design, final approval of manuscript; J.M.G.: conception and design, financial support, data analysis and interpretation, manuscript writing, and final approval of manuscript.

REFERENCES

1 White-Chu EF, Flock P, Struck B et al. Pressure ulcers in long-term care. Clin Geriatr Med 2011;27:241–258.

2 Wyndaele M, Wyndaele JJ. Incidence, prevalence and epidemiology of spinal cord injury: What learns a worldwide literature survey? Spinal Cord 2006;44:523–529.

3 Krause JS, Zhai Y, Saunders LL et al. Risk of mortality after spinal cord injury: An 8-year prospective study. Arch Phys Med Rehabil 2009;90:1708–1715.

4 Cao Y, Krause JS, DiPiro N. Risk factors for mortality after spinal cord injury in the USA. Spinal Cord 2013;51:413–418.

5 Black J, Baharestani M, Cuddigan J et al. National Pressure Ulcer Advisory Panel's updated pressure ulcer staging system. Urol Nurs 2007; 27:144–150, 156.

6 Clemens MW, Broyles JM, Le PN et al. Innovation and management of diabetic foot wounds. Surg Technol Int 2010;20:61–71.

7 Clemens MW, Attinger CE. Biological basis of diabetic foot wounds. Surg Technol Int 2008; 17:89–95.

8 Xie X, McGregor M, Dendukuri N. The clinical effectiveness of negative pressure wound therapy: A systematic review. J Wound Care 2010;19:490–495.

9 Cushing CA, Phillips LG. Evidence-based medicine: Pressure sores. Plast Reconstr Surg 2013;132:1720–1732.

10 Nguyen PK, Smith AL, Reynolds KJ. A literature review of different pressure ulcer models from 1942–2005 and the development of an ideal animal model. Australas Phys Eng Sci Med 2008;31:223–225.

11 Peirce SM, Skalak TC, Rodeheaver GT. Ischemia-reperfusion injury in chronic pressure ulcer formation: A skin model in the rat. Wound Repair Regen 2000;8:68–76.

12 Bouten CV, Oomens CW, Baaijens FP et al. The etiology of pressure ulcers: Skin deep or muscle bound? Arch Phys Med Rehabil 2003;84:616–619.

13 Wu Y, Wang J, Scott PG et al. Bone marrow-derived stem cells in wound healing: A review. Wound Repair Regen 2007;15(suppl 1):S18–S26.

14 Stadler I, Zhang RY, Oskoui P et al. Development of a simple, noninvasive, clinically relevant model of pressure ulcers in the mouse. J Invest Surg 2004;17:221–227.

15 Demiot C, Sarrazy V, Javellaud J et al. Erythropoietin restores C-fiber function and prevents pressure ulcer formation in diabetic mice. J Invest Dermatol 2011;131:2316–2322.

16 Park CJ, Clark SG, Lichtensteiger CA et al. Accelerated wound closure of pressure ulcers in aged mice by chitosan scaffolds with and without bFGF. Acta Biomater 2009;5:1926–1936.

17 Saito Y, Hasegawa M, Fujimoto M et al. The loss of MCP-1 attenuates cutaneous ischemia-reperfusion injury in a mouse model of pressure ulcer. J Invest Dermatol 2008;128:1838–1851.

18 Tong M, Tuk B, Hekking IM et al. Heparan sulfate glycosaminoglycan mimetic improves pressure ulcer healing in a rat model of cutaneous ischemia-reperfusion injury. Wound Repair Regen 2011;19:505–514.

19 Wassermann E, van Griensven M, Gstaltner K et al. A chronic pressure ulcer model in the nude mouse. Wound Repair Regen 2009;17:480–484.

20 Schatteman GC, Ma N. Old bone marrow cells inhibit skin wound vascularization. STEM CELLS 2006;24:717–721.

21 Gimble JM, Katz AJ, Bunnell BA. Adipose-derived stem cells for regenerative medicine. Circ Res 2007;100:1249–1260.

22 Nayeri F, Xu J, Abdiu A et al. Autocrine production of biologically active hepatocyte growth factor (HGF) by injured human skin. J Dermatol Sci 2006;43:49–56.

23 Amos PJ, Kapur SK, Stapor PC et al. Human adipose-derived stromal cells accelerate diabetic wound healing: Impact of cell formulation and delivery. Tissue Eng Part A 2010;16: 1595–1606.

24 Kilroy GE, Foster SJ, Wu X et al. Cytokine profile of human adipose-derived stem cells: Expression of angiogenic, hematopoietic, and proinflammatory factors. J Cell Physiol 2007;212: 702–709.

25 Yu G, Wu X, Dietrich MA et al. Yield and characterization of subcutaneous human adipose-derived stem cells by flow cytometric and adipogenic mRNA analyzes. Cytotherapy 2010;12:538–546.

26 Staszkiewicz J, Frazier TP, Rowan BG et al. Cell growth characteristics, differentiation frequency, and immunophenotype of adult ear mesenchymal stem cells. Stem Cells Dev 2010;19: 83–92.

27 Strong AL, Bowles AC, MacCrimmon CP et al. Characterization of a murine pressure ulcer model to assess the regenerative potential of adipose-derived stromal cells. Plast Reconstr Surg GO 2015;3:e334.

28 Woodbury MG, Houghton PE. Prevalence of pressure ulcers in Canadian healthcare settings. Ostomy Wound Manage 2004;50: 22–24, 26, 28, 30, 32, 34, 36–38.

29 Bourin P, Bunnell BA, Casteilla L et al. Stromal cells from the adipose tissue-derived stromal vascular fraction and culture expanded adipose tissue-derived stromal/stem cells: A joint statement of the International Federation for Adipose Therapeutics and Science (IFATS) and the International Society for Cellular Therapy (ISCT). Cytotherapy 2013;15:641–648.

30 McIntosh KR, Frazier T, Rowan BG et al. Evolution and future prospects of adipose-derived immunomodulatory cell therapeutics. Expert Rev Clin Immunol 2013;9:175–184.

31 Pachón-Peña G, Yu G, Tucker A et al. Stromal stem cells from adipose tissue and bone marrow of age-matched female donors display distinct immunophenotypic profiles. J Cell Physiol 2011;226:843–851.

32 Dominici M, Le Blanc K, Mueller I et al. Minimal criteria for defining multipotent mesenchymal stromal cells: The International Society for Cellular Therapy position statement. Cytotherapy 2006;8:315–317.

33 de la Garza-Rodea AS, Knaän-Shanzer S, van Bekkum DW. Pressure ulcers: Description of a new model and use of mesenchymal stem cells for repair. Dermatology 2011;223:266–284.

34 Gimble JM, Bunnell BA, Chiu ES et al. Concise review: Adipose-derived stromal vascular fraction cells and stem cells: Let's not get lost in translation. STEM CELLS 2011;29:749–754.

35 Gimble JM, Guilak F, Bunnell BA. Clinical and preclinical translation of cell-based therapies using adipose tissue-derived cells. Stem Cell Res Ther 2010;1:19.

36 Mesimäki K, Lindroos B, Törnwall J et al. Novel maxillary reconstruction with ectopic bone formation by GMP adipose stem cells. Int J Oral Maxillofac Surg 2009;38:201–209.

37 Sándor GK, Numminen J, Wolff J et al. Adipose stem cells used to reconstruct 13 cases with cranio-maxillofacial hard-tissue defects. STEM CELLS TRANSLATIONAL MEDICINE 2014;3:530–540.

38 Thesleff T, Lehtimäki K, Niskakangas T et al. Cranioplasty with adipose-derived stem cells and biomaterial: A novel method for cranial reconstruction. Neurosurgery 2011;68: 1535–1540.

39 Bura A, Planat-Benard V, Bourin P et al. Phase I trial: The use of autologous cultured adipose-derived stroma/stem cells to treat patients with non-revascularizable critical limb ischemia. Cytotherapy 2014;16:245–257.

40 Kurtzberg J, Prockop S, Teira P et al. Allogeneic human mesenchymal stem cell therapy (remestemcel-L, Prochymal) as a rescue agent for severe refractory acute graft-versus-host disease in pediatric patients. Biol Blood Marrow Transplant 2014;20:229–235.

41 Scruggs BA, Semon JA, Zhang X et al. Age of the donor reduces the ability of human adipose-derived stem cells to alleviate symptoms in the experimental autoimmune encephalomyelitis mouse model. STEM CELLS TRANSLATIONAL MEDICINE 2013;2:797–807.

42 Zhang X, Bowles AC, Semon JA et al. Transplantation of autologous adipose stem cells lacks therapeutic efficacy in the experimental autoimmune encephalomyelitis model. PLoS One 2014;9:e85007.

43 Cianfarani F, Toietta G, Di Rocco G et al. Diabetes impairs adipose tissue-derived stem cell function and efficiency in promoting wound healing. Wound Repair Regen 2013;21:545–553.

44 Driskell RR, Clavel C, Rendl M et al. Hair follicle dermal papilla cells at a glance. J Cell Sci 2011;124:1179–1182.

45 Schmidt BA, Horsley V. Intradermal adipocytes mediate fibroblast recruitment during skin wound healing. Development 2013;140: 1517–1527.

46 Rigotti G, Marchi A, Galie M et al. Clinical treatment of radiotherapy tissue damage by lipoaspirate transplant: A healing process mediated by adipose-derived adult stem cells. Plast Reconstr Surg 2007;119:1409–1404.

See www.StemCellsTM.com for supporting information available online.